

RO-FIGS: Efficient and Expressive Tree-Based Ensembles for Tabular Data

Urška Matjašec¹

Nikola Simidjievski^{2,1}

Mateja Jamnik¹

¹Department of Computer Science and Technology, ²PBCI, Department of Oncology

University of Cambridge, Cambridge, UK

{um234,ns779,mj201}@cam.ac.uk

Abstract—Tree-based models are often robust to uninformative features and can accurately capture non-smooth, complex decision boundaries. Consequently, they often outperform neural network-based models on tabular datasets at a significantly lower computational cost. Nevertheless, the capability of traditional tree-based ensembles to express complex relationships efficiently is limited by using a single feature to make splits. To improve the efficiency and expressiveness of tree-based methods, we propose Random Oblique Fast Interpretable Greedy-Tree Sums (RO-FIGS). RO-FIGS builds on Fast Interpretable Greedy-Tree Sums, and extends it by learning trees with oblique or multivariate splits, where each split consists of a linear combination learnt from random subsets of features. This helps uncover interactions between features and improves performance. The proposed method is suitable for tabular datasets with both numerical and categorical features. We evaluate RO-FIGS on 22 real-world tabular datasets, demonstrating superior performance and much smaller models over other tree- and neural network-based methods. Additionally, we analyse their splits to reveal valuable insights into feature interactions, enriching the information learnt from SHAP summary plots, and thereby demonstrating the enhanced interpretability of RO-FIGS models. The proposed method is well-suited for applications, where balance between accuracy and interpretability is essential.

Index Terms—tree-based ensembles, oblique trees, tabular data

I. INTRODUCTION

Current state-of-the-art methods for tabular data include gradient-boosted decision trees (GBDTs) [1]–[3] and several neural network-based methods such as FT-Transformer [4] and TabPFN [5]. However, no single method consistently outperforms the others [6]–[9]. We focus on improving tree-based methods since they often have a computational

advantage over complex neural networks with millions of parameters. Additionally, their hierarchical structure makes tree-based methods easier to comprehend than deep neural networks. Nevertheless, boosted ensembles, which iteratively add new trees to the model to correct the errors of previously built trees [1]–[3], can become complex with hundreds of trees and splits, making their interpretation challenging. Moreover, traditional splitting methods in boosted ensembles rely on single features, limiting the model’s ability to capture complex relationships between features.

To overcome these limitations, we introduce RO-FIGS: a random oblique fast interpretable greedy-tree sum method, which constructs splits as linear combinations of features, rather than considering only a singular feature to make a split. The splits reflect interactions among multiple features, which makes them more expressive than univariate splits. Moreover, RO-FIGS captures complex relationships between features more efficiently, as fewer splits are needed to represent complex patterns, leading to more compact models.

The structure of RO-FIGS builds on FIGS [10], which allows for constructing models in a flexible way as it can adapt to the additive structure if one exists in the data. However, it differs from FIGS due to the following technical novelties. First, RO-FIGS employs oblique splits, thereby enabling feature interaction directly within the splits. Second, it adopts a different stopping condition. Instead of strictly limiting the number of splits, RO-FIGS uses the minimum impurity decrease value to stop the training, which potentially yields larger models but also significantly improves the performance. Nevertheless, the size of both FIGS and RO-FIGS models remains comparable across most datasets.

We demonstrate the compactness of RO-FIGS models, consisting of up to only five trees and, with few exceptions, a low number of splits. This compact nature of RO-FIGS models not only improves their efficiency, which is measured as the balance between performance and compactness, but also makes them inherently more interpretable. Furthermore, by analysing linear combinations of features that often appear together in oblique splits, we offer a better understanding of the importance and interaction between features. We show that these splits are expressive and further enhance the interpretability of RO-FIGS. This suggests that RO-FIGS is well-suited for real-world scenarios, offering a good balance between performance and interpretability.

© 2025 IEEE. Personal use of this material is permitted. Permission from IEEE must be obtained for all other uses, in any current or future media, including reprinting/republishing this material for advertising or promotional purposes, creating new collective works, for resale or redistribution to servers or lists, or reuse of any copyrighted component of this work in other works.

UM is grateful to the Cambridge Commonwealth, European & International Trust for funding received as a DeepMind Cambridge Scholar to undertake her degree, and for the Trust’s and Google DeepMind’s support in publishing this article; UM also acknowledges the support from the Department of Computer Science and Technology, University of Cambridge, UK. NS and MJ acknowledge the support of the U.S. Army Medical Research and Development Command of the Department of Defense; through the FY22 Breast Cancer Research Program of the Congressionally Directed Medical Research Programs, Clinical Research Extension Award GRANT13769713. Opinions, interpretations, conclusions, and recommendations are those of the authors and are not necessarily endorsed by the Department of Defense.

The contributions of this paper are two-fold:

- 1) We introduce RO-FIGS, a novel and well-performing tree-based method, which builds an ensemble of oblique trees in an additive way (Section III). The implementation is available at: <https://github.com/um-k/rofigs>.
- 2) We demonstrate the capabilities of RO-FIGS in a series of experiments, showing they produce compact and performant models at lower computational cost, compared to many state-of-the-art methods for tabular data (Sections IV-B and IV-C). Further analysis reveals RO-FIGS’ interpretability properties beyond those produced by standard post-hoc approaches (such as SHAP), thus further enhancing our understanding of the model’s decision-making process (Section IV-D).

II. RELATED WORK

Greedy-tree sums: The foundation of our proposed method are greedy-tree sums (FIGS) [10], a generalisation of CART algorithm [11], which allows for building multiple trees in an additive way. This process involves creating new trees using the residuals of the preceding ones, much like GBDTs. However, FIGS adds one split to the model in each iteration, in contrast to GBDTs, which add the entire trees. There are two stopping criteria for FIGS: the number of trees and the total number of splits across all trees. FIGS outperforms traditional decision tree models, while at the same time building smaller, more compact models. Tan et al. [10] show that FIGS outperforms boosted stumps, but our experiments show that its performance is still subpar to traditional GBDTs like LightGBM [2] and CatBoost [3] (see Table I). The strict stopping conditions prevent FIGS from undergoing sufficient training, leading to its underperformance. Instead of applying strict constraints on the number of trees and splits in the model, RO-FIGS is more flexible and employs a minimum impurity decrease value to stop the training process.

Oblique trees: While traditional decision trees use a single feature in any splitting node, oblique or multivariate trees use a combination of features to define a split [11]–[13]. This makes them more expressive than univariate trees and enables them to learn similar decision boundaries with much shallower trees. However, oblique splits are more complex and can be harder to comprehend than univariate splits. This is especially pronounced when a split represents a linear combination of a substantial number of features. To reduce the complexity of splits, we use a hyperparameter to limit the number of features per split and employ further regularisation inside the splits.

Ensembles: Tree-based models hierarchically split the data based on feature values. Tree ensembles often achieve better performance and robustness by learning and combining many trees, either simultaneously (e.g., random forest [14]) or sequentially (e.g., FIGS [10], LightGBM [2]). RO-FIGS builds on sequential approaches, where new ensemble-constituent trees are learnt using the errors made by preceding trees, using their residuals. Ensembles of decision trees, both traditional and oblique, generally outperform single trees at the cost of

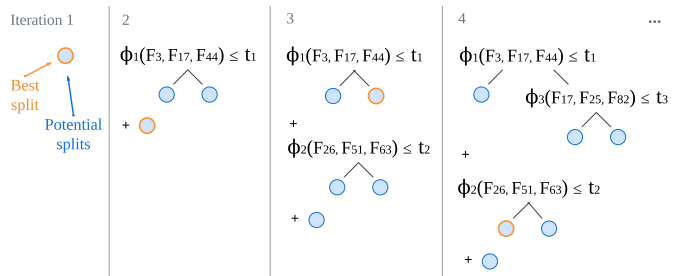


Fig. 1. Fitting process of RO-FIGS on a toy example. RO-FIGS adds one split to the model in each iteration. Splits are oblique and computed as linear combinations $\Phi()$ of multiple randomly selected features F . t denotes the threshold value for splitting. The figure has been adapted from [10].

increased model complexity and reduced interpretability. We avoid this problem by using regularisation within the splits.

Optimal trees: Unlike greedy algorithms that employ heuristics for tree construction, optimal tree methods [15]–[18] seek to learn the globally optimal trees, which can result in superior performance. However, their computational demand can often hinder their applicability to larger datasets. This limitation arises from the exhaustive search required to identify the best possible tree configuration. To mitigate this, some optimal tree methods [19]–[21] may introduce constraints that compromise optimality in favour of computational efficiency. While optimal trees are generally small in size, we show that RO-FIGS has a smaller trade-off between performance and both size and computational cost.

III. METHOD

We denote a training set as $D := \{(\mathbf{x}_i, y_i)\}_{i=1}^n$, where n is the number of samples and y_i are the corresponding labels that can be continuous values in regression tasks or binary labels (0 or 1) in binary classification tasks.

RO-FIGS leverages the concept of FIGS and constructs a flexible number of (usually a few) decision trees in summation. This means that at inference time, predictions are made by summing the predictions of all trees, while additionally applying a sigmoid function for classification tasks. The pseudocode of RO-FIGS is shown in Algorithm 1, and Fig. 1 illustrates the learning procedure in RO-FIGS.

In each iteration, RO-FIGS adds one split to the existing model (line 23). This split either replaces one of the current leaves or adds an additional stump to the model. At the start of every iteration, RO-FIGS randomly selects a subset of features that will be considered for learning splits in this iteration (line 11). The size of the subsets, which we refer to as *beams*, is determined by hyperparameter `BEAM_SIZE`, which can take any value between one and the number of all available features. At iteration i , there are $i + j$ potential splits, where j refers to the current number of trees in the model (lines 13–15). A potential split with the maximum impurity decrease is then added to the current model (lines 17 and 23). Due to the random feature selection, it is possible that only uninformative features are chosen. We, therefore, allow multiple repetitions per iteration. More specifically, if all $i + j$ potential splits have

Algorithm 1 RO-FIGS

```
1: Input: X: features, y: outcomes, BEAM_SIZE: number of considered features per split, MIN_IMP_DEC: minimum impurity decrease, MAX_SPLITS: maximum number of splits
2: trees = []
3: while (get_max_imp_dec() > MIN_IMP_DEC or first_iteration) and count_total_splits() < MAX_SPLITS do
4:   feat = select_random(BEAM_SIZE)
5:    $\Phi$  = compute_linear_combination(X, y, feat)
6:   all_trees = join(trees, define_oblique_split( $\Phi$ ))
7:   potential_splits = []
8:   for tree in all_trees do
9:     y_res = y - predict(all_trees except tree) // residuals
10:    for repetition in range(r) do
11:      feat = select_random(BEAM_SIZE)
12:      for leaf in tree do
13:         $\Phi$  = compute_linear_combination(X, y_res, feat)
14:        potential_split = define_oblique_split( $\Phi$ , leaf)
15:        potential_splits.append(potential_split)
16:      end for
17:      best_split = split_with_max_imp_dec(potential_splits)
18:      if impurity_decrease(best_split) > MIN_IMP_DEC then
19:        break
20:      end if
21:    end for
22:  end for
23:  trees.insert(best_split)
24: end while
25: Return: trees
```

impurity decrease lower than the minimum impurity decrease value (i.e., MIN_IMP_DEC; line 18), then another subset of features is randomly selected and evaluated. The process is repeated up to r times per iteration (line 10).

A. Split optimisation

Each potential split is an oblique stump computed on a random subset of features. A linear combination of k features is represented as $\Phi(F_1, \dots, F_k)$ (line 13, $k = \text{BEAM_SIZE}$). We use the implementation of Stepišnik and Kocev [22] (with the default hyperparameters, except for choosing one tree with depth one) to create splits with gradient-descent-based split learning. The computed splits take form of $w_1 * F_1 + \dots + w_k * F_k \leq t$, where w_1 and w_k represent weights, F_1 and F_k features, and t a threshold. The concrete steps of the split optimisation are as follows. First, the splitting features are randomly chosen (i.e., F_1, \dots, F_k). The objective function for the split optimisation is defined as

$$\min_{w,b} \|w\|_{1/2} + C * g(w, b), \quad (1)$$

where $\|w\|_{1/2} = (\sum_{i=1}^k \sqrt{|w_i|})^2$, k is the number of features, and C corresponds to the regularisation strength. $L_{\frac{1}{2}}$ norm induces weight sparsity and reduces split complexity, resulting in smaller splits. A fitness function g guides the optimisation process with the objective to minimise the impurity (defined as weighted variances) on both sides of the hyperplane.

B. Nominal features

We explore three encoding techniques for transforming nominal features (i.e., categorical features without an inher-

ent order) into numerical ones. The first approach, E-OHE, employs one-hot encoding, a common practice for handling nominal features [23]. The other two techniques, denoted as E-COUNT and E-PROP, are target encoding variants that leverage target information to transform nominal features into ordered ones in such an order that the target consistently changes [24]–[26]. Specifically, E-PROP orders categories based on the proportion of 1s in binary classification tasks (or by increasing mean in regression tasks), while E-COUNT simply counts 1s in the target variable. The main advantage of E-COUNT and E-PROP over E-OHE is that they do not increase the dimensionality of the data. However, E-OHE leads to best performance on average (see Table III in Appendix A-A¹), so we one-hot encode nominal features before passing them to RO-FIGS.

C. Hyperparameters and stopping conditions

RO-FIGS’s primary stopping condition is based on the minimum impurity decrease (i.e., MIN_IMP_DEC), a standard parameter in tree-based methods. More specifically, in the case of RO-FIGS, this is further regularised, where the training process stops if there is no significant impurity decrease (specified value) after r repeated attempts (five by default). Note that we did not observe any performance benefits when employing other criteria here, such as limiting the number of splits as in [10] (see Table VIII in Appendix B-B). RO-FIGS also employs a hyperparameter for BEAM_SIZE, which determines the size of the beam, that is, the number of features considered per split. This parameter influences the complexity of individual splits: larger values allow for more exploration but increase computational cost, while smaller values may restrict optimal splits.

IV. EXPERIMENTS

We quantitatively evaluate RO-FIGS (Section IV-B) and discuss the efficiency of tree-based models by analysing the balance between their accuracy and size (Section IV-C). We inspect oblique splits to show the expressiveness and enhanced interpretability of RO-FIGS models (Section IV-D).

A. Experimental setup

a) *Datasets:* Our choice of datasets is guided by a recent study about tabular data [9]. We choose 22 binary classification datasets with varying numbers of features and samples from OpenML. We first split the data according to 10 train/test folds provided by OpenML, which enables the comparison of our results on the test data with other works. Furthermore, we split each training fold into training and validation sets, using the same splits as [9]. Refer to Appendix A-A for further details on the datasets (Table II) and preprocessing.

¹Supplementary material containing all appendices is available at: <https://github.com/um-k/rofigs>.

TABLE I

CLASSIFICATION PERFORMANCE OF RO-FIGS AND 10 BASELINES ON 22 TABULAR DATASETS. WE REPORT MEAN \pm STD OF THE TEST BALANCED ACCURACY ACROSS 10 FOLDS, AND AVERAGE RANK ACROSS ALL DATASETS. NOTE THAT WE USE REVERSED RANK (WHERE HIGHER IS BETTER). WE HIGHLIGHT THE **FIRST**, **SECOND**, AND **THIRD** HIGHEST ACCURACY FOR EACH DATASET. RO-FIGS IS AMONGST THE TOP THREE ON 11 DATASETS AND RANKS THE BEST OVERALL.

Dataset	DT	MT	OT	ODT	RF	ETC	CatBoost	FIGS	Ens-ODT	MLP	RO-FIGS
blood	63.3 \pm 7.3	64.5 \pm 2.6	64.1 \pm 3.6	61.5 \pm 8.9	63.0 \pm 5.6	58.0 \pm 5.6	60.3 \pm 5.8	65.0 \pm 4.9	62.8 \pm 4.4	55.8 \pm 5.1	68.5 \pm 4.1
diabetes	70.8 \pm 4.9	68.5 \pm 5.8	71.0 \pm 7.1	69.7 \pm 8.3	72.6 \pm 5.7	72.5 \pm 6.2	70.5 \pm 7.0	70.2 \pm 4.8	69.9 \pm 4.8	70.6 \pm 6.5	73.6 \pm 4.7
breast-w	93.5 \pm 3.0	96.5 \pm 2.0	93.9 \pm 2.2	93.4 \pm 4.0	95.8 \pm 1.8	96.5 \pm 1.6	95.9 \pm 2.8	94.4 \pm 2.4	96.2 \pm 1.5	96.1 \pm 1.5	96.5 \pm 1.9
ilpd	56.0 \pm 4.1	57.3 \pm 5.5	52.0 \pm 3.8	54.2 \pm 10.0	56.6 \pm 6.9	54.6 \pm 4.9	58.9 \pm 6.8	53.2 \pm 7.3	59.8 \pm 4.9	51.6 \pm 3.7	61.9 \pm 10.4
monks2	94.6 \pm 4.8	87.1 \pm 8.9	52.8 \pm 5.4	86.8 \pm 14.6	74.9 \pm 6.3	91.1 \pm 5.3	78.3 \pm 8.1	63.7 \pm 7.6	98.1 \pm 2.5	99.9 \pm 0.1	99.5 \pm 0.8
climate	69.4 \pm 11.6	69.8 \pm 6.3	62.9 \pm 10.9	71.4 \pm 11.1	51.0 \pm 3.2	50.0 \pm 0.0	68.1 \pm 10.7	64.8 \pm 10.8	71.2 \pm 12.2	76.8 \pm 12.5	73.1 \pm 15.6
kc2	72.4 \pm 10.0	66.6 \pm 6.8	70.2 \pm 6.8	68.6 \pm 9.2	72.1 \pm 6.0	67.1 \pm 9.0	69.2 \pm 7.5	72.8 \pm 10.5	69.6 \pm 6.2	69.6 \pm 7.3	77.6 \pm 7.9
pc1	60.4 \pm 4.9	53.1 \pm 4.7	56.6 \pm 7.4	58.5 \pm 7.5	56.9 \pm 5.7	56.4 \pm 6.8	61.2 \pm 9.4	56.4 \pm 5.5	60.0 \pm 5.3	50.5 \pm 1.7	66.6 \pm 7.2
kc1	60.8 \pm 3.3	58.7 \pm 4.2	58.7 \pm 3.9	55.8 \pm 5.8	60.5 \pm 4.7	59.2 \pm 5.6	65.0 \pm 3.3	59.0 \pm 4.9	60.3 \pm 4.2	57.9 \pm 3.5	64.9 \pm 4.9
heart	80.0 \pm 6.9	78.2 \pm 6.2	82.5 \pm 4.4	77.8 \pm 5.8	82.5 \pm 7.5	82.7 \pm 7.5	83.3 \pm 5.2	81.2 \pm 7.6	84.2 \pm 8.4	82.5 \pm 6.4	84.8 \pm 6.4
tictactoe	92.2 \pm 2.5	97.6 \pm 1.8	67.6 \pm 3.7	86.7 \pm 7.0	95.9 \pm 4.3	97.4 \pm 3.2	99.9 \pm 0.1	84.3 \pm 5.7	97.1 \pm 2.5	97.5 \pm 1.7	94.4 \pm 3.1
wdbc	91.8 \pm 4.3	95.2 \pm 3.8	92.0 \pm 4.2	95.4 \pm 3.8	94.6 \pm 3.5	94.3 \pm 3.2	96.3 \pm 2.4	92.6 \pm 3.5	95.8 \pm 3.7	97.2 \pm 3.1	95.6 \pm 3.5
churn	84.2 \pm 1.8	82.9 \pm 2.1	67.5 \pm 1.7	86.7 \pm 1.8	83.8 \pm 2.1	74.4 \pm 3.2	88.3 \pm 1.9	82.6 \pm 3.6	87.8 \pm 2.4	84.8 \pm 3.6	86.3 \pm 2.0
pc3	58.3 \pm 4.4	59.7 \pm 6.1	52.3 \pm 2.7	56.8 \pm 6.3	52.3 \pm 3.3	52.0 \pm 2.4	60.7 \pm 6.5	54.4 \pm 4.6	55.6 \pm 4.1	50.0 \pm 0.0	62.9 \pm 6.6
biodeg	78.3 \pm 4.0	82.1 \pm 3.0	76.5 \pm 4.5	79.4 \pm 2.7	82.0 \pm 3.1	81.4 \pm 4.9	85.3 \pm 2.7	76.6 \pm 5.1	83.9 \pm 4.2	86.2 \pm 5.6	82.7 \pm 3.7
credit	83.9 \pm 3.8	82.0 \pm 3.9	85.4 \pm 4.0	84.3 \pm 3.7	86.4 \pm 5.2	86.1 \pm 4.2	86.8 \pm 4.4	85.4 \pm 3.3	85.9 \pm 4.4	85.8 \pm 3.1	85.7 \pm 5.2
spambase	90.4 \pm 2.1	91.4 \pm 1.9	87.9 \pm 2.4	91.9 \pm 1.9	93.3 \pm 2.0	92.5 \pm 2.6	94.9 \pm 1.2	89.8 \pm 2.8	94.6 \pm 1.5	92.5 \pm 2.0	92.9 \pm 1.3
credit-g	63.3 \pm 6.3	65.2 \pm 5.7	58.5 \pm 3.7	64.2 \pm 8.2	63.4 \pm 5.6	63.6 \pm 7.5	66.8 \pm 4.9	62.1 \pm 5.4	67.7 \pm 4.7	68.8 \pm 5.4	65.7 \pm 5.0
friedman	84.9 \pm 6.7	69.8 \pm 4.7	80.4 \pm 6.6	61.2 \pm 7.5	77.8 \pm 5.3	68.5 \pm 5.8	86.4 \pm 8.7	82.0 \pm 4.8	61.5 \pm 8.3	59.8 \pm 8.4	80.0 \pm 7.4
usps	93.4 \pm 2.9	98.5 \pm 1.2	92.3 \pm 1.6	96.6 \pm 1.4	97.2 \pm 1.4	97.5 \pm 1.2	98.0 \pm 1.5	93.5 \pm 2.2	97.8 \pm 1.7	98.0 \pm 1.1	97.5 \pm 1.6
bioresponse	71.8 \pm 1.5	71.3 \pm 3.2	71.0 \pm 2.1	72.3 \pm 2.2	78.9 \pm 2.1	78.1 \pm 2.0	77.7 \pm 3.3	72.6 \pm 2.9	78.1 \pm 2.6	74.6 \pm 3.0	72.9 \pm 2.6
speeddating	63.8 \pm 3.3	64.0 \pm 1.1	60.1 \pm 3.0	58.9 \pm 9.3	58.0 \pm 1.5	57.4 \pm 1.7	69.1 \pm 1.9	65.5 \pm 2.8	65.8 \pm 2.1	71.2 \pm 2.7	65.4 \pm 1.9
Avg. rank	5.3	5.5	3.4	4.3	6.1	5.3	8.5	4.5	7.8	6.5	8.8

b) *Baselines*: We compare RO-FIGS to several tree-based methods, including: decision tree [11], random forest [14], extremely randomised or extra trees (ETC) [27], FIGS [10], oblique decision tree (ODT) [22] and ensemble of oblique decision trees (Ens-ODT) [22], optimal tree (OT) [28], model tree (MT) [29], as well as several gradient-boosted ensembles (LightGBM [2], XGBoost [1] and CatBoost [3]). We present only the results of CatBoost as the top-performing GBDT baseline. Further results on the performance of the other two are given in Appendix B-A (Table VI). We also include an MLP with two hidden layers as a neural network baseline. Note that we also compared RO-FIGS to TabPFN [5], a recently proposed transformer-based approach tailored for tabular data tasks. However, since TabPFN has been pre-trained on some of the datasets we use for evaluation, we include this analysis in Appendix B-A (Table VII), as a direct comparison would be biased due to data leakage.

c) *Hyperparameter optimisation*: For tuning RO-FIGS, we perform a grid search over the parameters that control the impurity decrease and the size of the beam. More details can be found in Appendix A-B. We use hyperopt [30] to tune the hyperparameters of the baselines. The configuration, which leads to the best performance on validation data, is then used to train final models on the joint training data (comprising training and validation sets), and their performance on the hold-out test set is reported. The exception is the MLP baseline, which requires validation data for early stopping. We use 30 iterations of tuning for all methods except model trees, which we limit to five iterations due to a high computational overhead.

d) *Metrics*: To evaluate performance, we measure the balanced accuracy on the test split. We perform a 10-fold cross-validation and report the mean \pm standard deviation, averaged across 10 folds. We also report the mean rank of each method, ranked according to their performance, with higher ranks denoting better performance. To demonstrate the compactness of RO-FIGS models, we follow Tan et al. [10] and compute the number of splits and trees, which allows us to make further comparisons among tree-based models. These two reflect the model complexity and thus implicitly measure interpretability, as we assume more compact models to be more interpretable. Note that we do not explicitly analyse the depth of the trees, as we found it to be unreliable for measuring model complexity given different tree-learning methods. As a measure of efficiency, we also assess the balance between performance and compactness of tree-based models. Finally, we analyse oblique splits in RO-FIGS models to demonstrate their expressiveness. By identifying combinations of features that often appear together in the splits, we show which feature interactions positively contribute to the model’s performance. We analyse this data along with SHAP plots, which provide post-hoc model explainability.

B. How accurate are RO-FIGS models?

Table I shows that RO-FIGS, in general, is able to outperform all baselines. It consistently dominates on smaller datasets, performing comparably to other tree-based ensembles on datasets with a larger number of samples or features. The neural network baseline, MLP, is competitive, achieving top

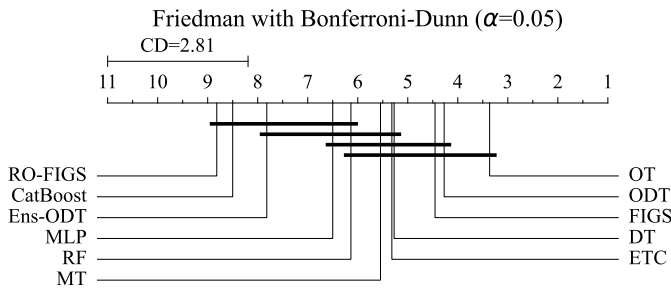


Fig. 2. Comparison of the average ranks of model performance, comparing RO-FIGS against the baselines, with respect to the Friedman statistical test followed by the Bonferroni-Dunn post-hoc test ($p < 0.05$). RO-FIGS ranks best (higher values are better), and statistically significantly better (outside the CD interval) than FIGS and five other baseline methods: MT, ETC, DT, ODT and OT.

performance on six datasets, but its rank is diminished due to poor performance on a few datasets (e.g., *pc1* and *friedman*).

To further assess the performance differences of the evaluated methods, we follow a standard statistical procedure recommended by Demšar [31]. We employ the corrected [32] Friedman statistical test [33] to determine the performance difference between RO-FIGS and the baselines. This is followed by the Bonferroni-Dunn [34] post-hoc test to identify which differences are statistically significant. Fig. 2 depicts the critical difference diagram (with a significance level threshold set at 95%, $p = 0.05$). RO-FIGS ranks best amongst all methods (higher values are better), and statistically significantly better than FIGS as well as other baselines outside the marked interval (for critical distance $CD = 2.81$), which includes MT, ETC, DT, ODT, and OT. Note that, while RO-FIGS ranks better than CatBoost, Ens-ODT, MLP, and RF, this difference is not statistically significant.

Oblique splits in RO-FIGS models are beneficial for performance. We attribute this to oblique splits not being restricted to splitting along a single feature dimension. This flexibility allows them to capture more intricate, non-linear relationships between features, leading to better-performing models. We observe that, with the exception of two datasets, RO-FIGS always outperforms FIGS, suggesting that while both methods benefit from the additive structure, RO-FIGS’s superior performance stems from using oblique splits. This comparison and further study on how varying the size of the beam (`BEAM_SIZE` parameter) influences the performance of RO-FIGS models is discussed in Appendix B-B.

C. How efficient are RO-FIGS models?

We assess efficiency as the balance between performance and compactness of the models. Since we cannot directly compare the compactness of tree- and network-based models, we exclude the MLP baseline from this analysis. We acknowledge, however, that neural networks have millions of parameters and thus offer very limited interpretability for their decisions.

We first use two quantitative measures to assess the size of RO-FIGS models: the number of trees and the total number

of splits across all trees. We then analyse the balance between each measure and the mean accuracy. This analysis provides an overview of potential trade-offs between compactness and performance, which is crucial in practical applications.

RO-FIGS produces performant small-sized models.

Fig. 3 (left and middle) shows a comparison between the size of tree-based models and their performance. The ideal, most efficient model would be positioned in the top-left corner, achieving the best accuracy whilst being compact. It is evident that RO-FIGS offers the best balance: it builds small and therefore more interpretable models, whilst outperforming the baselines. While RO-FIGS and CatBoost (which ranks second to our method) achieve similar average performance, the former builds much smaller models and is, therefore, more suitable for applications where simpler, more interpretable models are desired [35]. Further details are provided in Appendix B-C.

RO-FIGS is able to take advantage of the additive structure of the data, if that exists, and build multiple trees in summation. Our experiments show that it generates compact, yet high-performing, models. They consist of less than five trees on average, which is comparable to that of FIGS and much lower than ensembles (see Table IX in Appendix B-C). Moreover, we observe that both FIGS and RO-FIGS build either exactly one tree or multiple trees on most datasets. This confirms that both methods uncover the additive nature of the data if present. Overall, RO-FIGS builds models with a small number of trees.

With regards to the number of splits, RO-FIGS builds models with fewer than 15 splits on 15 datasets (see Table X in Appendix B-C). Furthermore, on 10 of these datasets, they have fewer than five splits. As with trees, the number of splits is comparable to FIGS, with few exceptions. Note that, in our analysis, we limited the maximum number of splits in FIGS to 20, as in [10], so it is likely that other methods will create models with more splits, especially on harder tasks. RO-FIGS models have even fewer splits than single decision trees on more than half of the datasets while performing much better. Tree ensembles, as expected, exhibit orders of magnitude more splits than a single tree- and FIGS-based models. Overall, RO-FIGS builds models with a low number of splits.

We have shown that RO-FIGS leads to good and stable performance with compact models. However, there is a trade-off between predictive performance and computational cost for training the models (see Fig. 3 (right)). Compared to other ensemble baselines, RO-FIGS may require more training time due to its on-the-fly learning and evaluation of oblique splits. Therefore, in scenarios with high-dimensional datasets, RO-FIGS can scale poorly with the number of potential splits and the size of the beam `BEAM_SIZE` (i.e., size of the feature sets). More specifically, in the worst case, the complexity of RO-FIGS is $\mathcal{O}(irm^2n^2d)$, where m, n, d, i , and r denote the number of splits, samples, features, gradient descent iterations (100 by default), and repetitions (five by default), respectively. RO-FIGS depends on the optimisation procedure for learning the splits, typically using a subset of d (i.e., `BEAM_SIZE`) features at every split. This process could be improved by computing potential splits within each iteration in parallel and

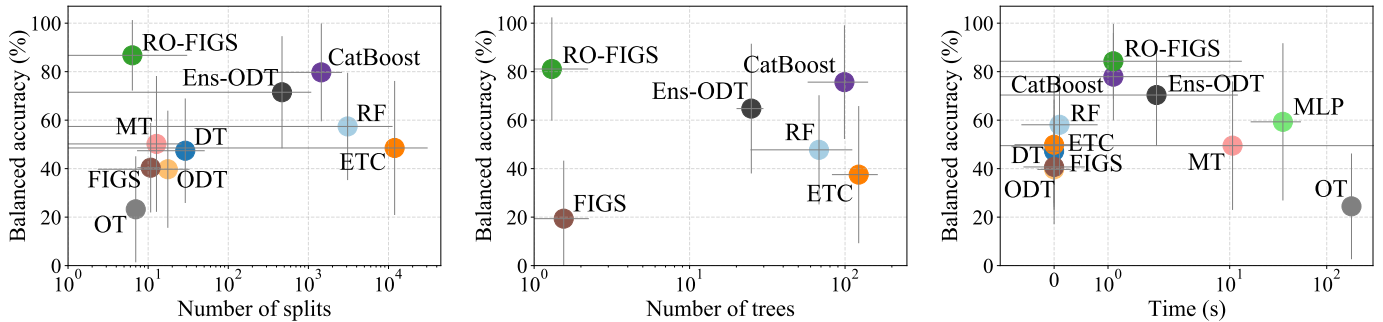


Fig. 3. Left and middle: Comparison between the performance and the number of splits and trees in tree-based models. RO-FIGS models achieve the best balance, as they are well-performing and small in size. Right: Comparison between the performance and training time. RO-FIGS offers a good balance between performance and computational cost. Performance is calculated as mean normalised accuracy for each method, over all datasets, with error bars spanning the 20th/80th percentile over all datasets. Note the logarithmic scale on the x-axes and the omission of single-tree methods in the middle figure.

using more effective heuristics or domain-specific knowledge for feature selection. Nevertheless, RO-FIGS still offers a favourable balance between practical time complexity and performance.

D. How expressive are RO-FIGS models?

To demonstrate the expressiveness of RO-FIGS models, we now analyse their oblique splits. First, we inspect the average number of features per split, which is constrained by the size of the beam (`BEAM_SIZE`). Due to the $L_{\frac{1}{2}}$ norm in (1), the number of features with non-zero weights is usually much lower than this upper limit, keeping the size of individual splits relatively small (see Table V in Appendix A-B for more details). A low number of features decreases the complexity of individual splits, making them more comprehensible and interpretable. This behaviour also suggests that RO-FIGS can, like other tree-based methods, recognise more informative features.

Next, we showcase the expressiveness of RO-FIGS models by analysing their splits on the *diabetes* dataset with eight features. Across all folds, RO-FIGS models consist of one tree with one split. Moreover, all splits consist of a linear combination of three features: *glucose*, *age*, and *BMI*. This is consistent with the SHAP summary plot of the RO-FIGS model (on the first fold), shown in Fig. 4, which shows

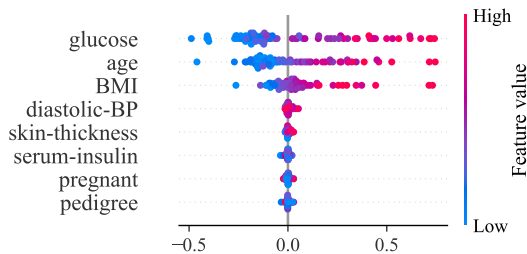


Fig. 4. SHAP summary plot of RO-FIGS on the *diabetes* dataset (fold 0). Similar to the baselines, *glucose*, *age*, and *BMI* features are contributing to the model the most. RO-FIGS with the accuracy of 73.6% (see Table I) outperforms all baselines on this dataset with only one split, demonstrating that a linear combination of features *glucose*, *age*, and *BMI* is optimal.

that only these features contribute to the model’s predictions. For comparison, SHAP plots of the baselines also identify these three features as very important. However, unlike other methods, RO-FIGS has the unique advantage of inherently capturing feature interactions within splits (as they are defined as linear combinations of features, Φ), thereby providing insights into specific interactions between features. More details can be found in Appendix B-D.

Overall, RO-FIGS consistently builds splits with multiple features and helps uncover important relationships between features. These results demonstrate that splits in RO-FIGS are more expressive and informative than univariate splits while considering a reasonable number of features at once. Furthermore, RO-FIGS models can provide additional information about the feature interactions that cannot be learnt from analysing splits of tree-based models with univariate splits or post-hoc explanation tools such as SHAP alone.

E. Limitations

RO-FIGS demonstrates good predictive performance while producing compact and interpretable models. Nevertheless, we acknowledged a few limitations related to its scalability to larger datasets and versatility to mixed-type tabular datasets. Future work includes exploring more efficient approaches for feature construction and selection, which will serve as the basis for learning oblique trees from numerical and nominal features, but also for reducing the computational burden for learning performant RO-FIGS.

V. CONCLUSION

In this work, we introduced RO-FIGS, a tree-based method for tabular data. RO-FIGS builds compact models with multiple trees by using residuals of previous trees. Its splits are oblique and expressed as linear combinations of multiple features, learnt from random subsets of features. We show that RO-FIGS achieves the highest average performance, surpassing both traditional tree-based methods and MLP, whilst building much smaller models. Due to the nature of oblique splits in RO-FIGS, we provide insights into the interactions between features that contribute to the models’ performance. We show

that this information enriches insights from SHAP summary plots, enhancing the interpretability of RO-FIGS. Although we focus on classification tasks in this work, the method is also applicable to regression tasks. The proposed method is especially well-suited for real-world applications, where the balance between accuracy and interpretability is crucial.

REFERENCES

- [1] T. Chen and C. Guestrin, "XGBoost: A scalable tree boosting system," in *Proceedings of the 22nd ACM SIGKDD International Conference on Knowledge Discovery and Data Mining*, ser. KDD '16. New York, NY, USA: Association for Computing Machinery, 2016, p. 785–794.
- [2] G. Ke, Q. Meng, T. Finley, T. Wang, W. Chen, W. Ma, Q. Ye, and T.-Y. Liu, "LightGBM: A highly efficient gradient boosting decision tree," in *Proceedings of the 31st International Conference on Neural Information Processing Systems*, ser. NIPS'17. Red Hook, NY, USA: Curran Associates Inc., 2017, p. 3149–3157.
- [3] L. Prokhorenkova, G. Gusev, A. Vorobev, A. V. Dorogush, and A. Gulin, "CatBoost: Unbiased boosting with categorical features," in *Proceedings of the 32nd International Conference on Neural Information Processing Systems*, ser. NIPS'18. Red Hook, NY, USA: Curran Associates Inc., 2018, p. 6639–6649.
- [4] Y. Gorishniy, I. Rubachev, V. Khruikov, and A. Babenko, "Revisiting deep learning models for tabular data," in *Advances in Neural Information Processing Systems*, M. Ranzato, A. Beygelzimer, Y. Dauphin, P. Liang, and J. W. Vaughan, Eds., vol. 34. Curran Associates, Inc., 2021, pp. 18932–18943.
- [5] N. Hollmann, S. Müller, K. Eggensperger, and F. Hutter, "TabPFN: A transformer that solves small tabular classification problems in a second," in *The Eleventh International Conference on Learning Representations*, 2023.
- [6] R. Shwartz-Ziv and A. Armon, "Tabular data: Deep learning is not all you need," *arXiv preprint arXiv:2106.03253*, 2021.
- [7] V. Borisov, T. Leemann, K. Seßler, J. Haug, M. Pawelczyk, and G. Kasneci, "Deep neural networks and tabular data: A survey," *IEEE Transactions on Neural Networks and Learning Systems*, pp. 1–21, 2022.
- [8] L. Grinsztajn, E. Oyallon, and G. Varoquaux, "Why do tree-based models still outperform deep learning on typical tabular data?" in *Thirty-sixth Conference on Neural Information Processing Systems Datasets and Benchmarks Track*, 2022.
- [9] D. McElfresh, S. Khandagale, J. Valverde, V. P. C, G. Ramakrishnan, M. Goldblum, and C. White, "When do neural nets outperform boosted trees on tabular data?" *arXiv preprint arXiv:2305.02997*, 2023.
- [10] Y. S. Tan, C. Singh, K. Nasser, A. Agarwal, and B. Yu, "Fast interpretable greedy-tree sums," *arXiv preprint arXiv:2201.11931*, 2022.
- [11] L. Breiman, J. Friedman, C. J. Stone, and R. Olshen, *Classification and Regression Trees*. CRC press, 1984.
- [12] S. K. Murthy, S. Kasif, and S. Salzberg, "A system for induction of oblique decision trees," *Journal of Artificial Intelligence Research* 2, vol. 2, no. 1, pp. 1–32, 1994.
- [13] B.-B. Yang, S.-Q. Shen, and W. Gao, "Weighted oblique decision trees," *Proceedings of the AAAI Conference on Artificial Intelligence*, vol. 33, no. 1, pp. 5621–5627, 2019.
- [14] L. Breiman, "Random forests," *Machine Learning*, vol. 45, no. 1, pp. 5–32, 2001.
- [15] D. Bertsimas and J. Dunn, "Optimal classification trees," *Machine Learning*, vol. 106, no. 7, pp. 1039–1082, 2017.
- [16] S. Nijssen and E. Fromont, "Optimal constraint-based decision tree induction from itemset lattices," *Data Mining and Knowledge Discovery*, vol. 21, no. 1, pp. 9–51, 2010.
- [17] S. Verwer and Y. Zhang, "Learning optimal classification trees using a binary linear program formulation," *Proceedings of the AAAI Conference on Artificial Intelligence*, vol. 33, no. 1, pp. 1625–1632, 2019.
- [18] J. Lin, C. Zhong, D. Hu, C. Rudin, and M. Seltzer, "Generalized and scalable optimal sparse decision trees," in *Proceedings of the 37th International Conference on Machine Learning*, ser. ICML'20. JMLR.org, 2020.
- [19] N. Narodytska, A. Ignatiev, F. Pereira, and J. Marques-Silva, "Learning optimal decision trees with SAT," in *Proceedings of the Twenty-Seventh International Joint Conference on Artificial Intelligence, IJCAI-18*. International Joint Conferences on Artificial Intelligence Organization, 7 2018, pp. 1362–1368.
- [20] F. Avellaneda, "Efficient inference of optimal decision trees," *Proceedings of the AAAI Conference on Artificial Intelligence*, vol. 34, no. 4, pp. 3195–3202, 2020.
- [21] M. Firat, G. Crognier, A. F. Gabor, C. Hurkens, and Y. Zhang, "Column generation based heuristic for learning classification trees," *Computers & Operations Research*, vol. 116, p. 104866, 2020.
- [22] T. Stepišnik and D. Kocev, "Oblique predictive clustering trees," *Knowledge-Based Systems*, vol. 227, p. 107228, 2021.
- [23] F. Pedregosa, G. Varoquaux, A. Gramfort, V. Michel, B. Thirion, O. Grisel, M. Blondel, P. Prettenhofer, R. Weiss, V. Dubourg, J. Vanderplas, A. Passos, D. Cournapeau, M. Brucher, M. Perrot, and E. Duchesnay, "Scikit-learn: Machine learning in Python," *Journal of Machine Learning Research*, vol. 12, pp. 2825–2830, 2011.
- [24] D. Micci-Barreca, "A preprocessing scheme for high-cardinality categorical attributes in classification and prediction problems," *SIGKDD Explor. Newsl.*, vol. 3, no. 1, p. 27–32, 2001.
- [25] M. N. Wright and I. R. König, "Splitting on categorical predictors in random forests," *PeerJ*, vol. 7, p. e6339, Feb 2019.
- [26] W. Zhu, R. Qiu, and Y. Fu, "Comparative study on the performance of categorical variable encoders in classification and regression tasks," Preprint arXiv:2401.09682, 2024.
- [27] P. Geurts, D. Ernst, and L. Wehenkel, "Extremely randomized trees," *Machine Learning*, vol. 63, no. 1, pp. 3–42, 2006.
- [28] B. Tang, "Optimal classification trees," 2021. [Online]. Available: https://github.com/LucasBoTang/Optimal_Classification_Trees
- [29] M. Cerliani, "linear-tree 0.3.5," 2022. [Online]. Available: <https://pypi.org/project/linear-tree>
- [30] J. Bergstra, D. Yamins, and D. Cox, "Making a science of model search: Hyperparameter optimization in hundreds of dimensions for vision architectures," in *Proceedings of the 30th International Conference on Machine Learning*, ser. Proceedings of Machine Learning Research, S. Dasgupta and D. McAllester, Eds., vol. 28, no. 1. Atlanta, Georgia, USA: PMLR, 17–19 Jun 2013, pp. 115–123.
- [31] J. Demšar, "Statistical comparisons of classifiers over multiple data sets," *Journal of Machine Learning Research*, vol. 7, no. 1, pp. 1–30, 2006.
- [32] R. L. Iman and J. M. Davenport, "Approximations of the critical region of the fbiectan statistic," *Communications in Statistics - Theory and Methods*, vol. 9, no. 6, pp. 571–595, 1980.
- [33] M. Friedman, "A comparison of alternative tests of significance for the problem of m rankings," *The Annals of Mathematical Statistics*, vol. 11, no. 1, pp. 86 – 92, 1940.
- [34] O. J. Dunn, "Multiple comparisons among means," *Journal of the American Statistical Association*, vol. 56, no. 293, pp. 52–64, 1961.
- [35] C. Rudin, "Stop explaining black box machine learning models for high stakes decisions and use interpretable models instead," *Nature Machine Intelligence*, vol. 1, pp. 206–215, 2019.

Supplementary material for RO-FIGS: Efficient and Expressive Tree-Based Ensembles for Tabular Data

Urška Matjašec¹

Nikola Simidjievski^{2,1}

Mateja Jamnik¹

¹Department of Computer Science and Technology, ²PBCI, Department of Oncology
University of Cambridge, Cambridge, UK
{um234,ns779,mj201}@cam.ac.uk

APPENDIX A

EXTENDED EXPERIMENTAL SETUP

Here, we give more details about the datasets used for evaluation (see Table II), discuss different encodings of nominal features in RO-FIGS (see Table III), and provide details about the search space for hyperparameter tuning of the tree-based baselines (see Table IV) and grid search space along with the best per-dataset configuration for RO-FIGS (see Table V).

A. Datasets

All datasets are publicly available on OpenML and summarised in Table II. We first split the data according to 10 train/test folds provided by OpenML and then split each training fold into training and validation sets, using the same splits as McElfresh et al. [9]. Each dataset is therefore split into training (80%), validation (10%), and test (10%) sets.

Most baselines expect numerical input, therefore we one-hot encode nominal features. The only exceptions are CatBoost and LightGBM, to which we pass the indices of nominal features. For RO-FIGS, we evaluate three encoding approaches of transforming nominal features into numerical: E-OHE, E-COUNT, and E-PROP, as computing linear combinations of nominal features is not trivial. Table III demonstrates that one-hot encoding outperforms the other two, which transform nominal features into ordered ones without increasing the dimensionality of the data. Therefore, we use one-hot encoding to transform nominal features into numerical ones.

The data is min-max scaled to $[0, 1]$. Specifically, during hyperparameter tuning (with models trained on the training data and evaluated on the validation data), the scaling transformation is learnt from the training data and applied to the validation data. When training the final model on the combined training and validation data (and evaluated on test data), the transformation learnt from the joint dataset is applied to the test data.

B. Hyperparameter tuning

a) Baselines: We employ `hyperopt` [30] with the tree-structured Parzen estimator to fine-tune hyperparameters for the tree-based baselines. Each baseline undergoes 30 tuning iterations, with the exception of the model tree, which is limited to five iterations due to its high computational cost. The details about the search space of hyperparameters are shown in Table IV. TabPFN requires no tuning and we use its default hyperparameter values. For optimal trees, we set the depth to three and trained each model for up to three minutes.

Because we compare RO-FIGS to the baselines w.r.t. the number of trees and splits, we additionally introduce the following penalties to promote the compactness in the tree-based baselines:

- **DT:** $0.001 \times \text{max_depth}$
- **MT** using `RidgeClassifier` as the base estimator: $0.001 \times \text{max_depth}$
- **ODT:** $0.001 \times \text{max_depth}$
- **RF, ETC, CatBoost, LightGBM, XGBoost:** $0.001 \times \text{max_depth} + 0.0001 \times \text{n_estimators}$
- **FIGS:** $0.001 \times \text{max_rules} + 0.001 \times \text{max_trees}$
- **Ens-ODT:** $0.001 \times \text{max_depth} + 0.0001 \times \text{num_trees}$

b) RO-FIGS: To better understand the behaviour of RO-FIGS models across a spectrum of hyperparameter values, we perform a grid search over two hyperparameters: `BEAM_SIZE`, which limits the number of features considered per split, and `MIN_IMP_DEC`, defining the stopping condition for training. We use a constant search space for the minimum impurity decrease parameter and tailor the other parameter to the number of features in the dataset (i.e., d):

- `MIN_IMP_DEC:` 0.05, 0.1, 1, 5, 10, and
- `BEAM_SIZE:` 1, 2, \sqrt{d} , $\frac{d}{4}$, $\frac{d}{2}$, d ; where d is the total number of features in a dataset.

The middle two columns in Table V show the optimal configuration, which leads to the best performance on the test data. It should be noted that the BEAM_SIZE value is the maximum number of features that RO-FIGS considers at each iteration. In practice, only a small proportion of features have non-zero weights, leading to a much lower average number of features per split. This is reported in the last column of Table V.

TABLE II
 PROPERTIES OF THE BENCHMARK DATASETS FOR BINARY CLASSIFICATION TASKS. *Nominal* INDICATES THE NUMBER OF NOMINAL CATEGORICAL FEATURES, WHILE *Final* SHOWS THE TOTAL NUMBER OF FEATURES AFTER NOMINAL FEATURES HAVE BEEN ONE-HOT ENCODED (DATASETS ARE ORDERED W.R.T. THE LATTER).

Dataset	Original name (OpenML id)	Numerical	Nominal	Final	Samples
blood	blood-transfusion-service-center (1464)	4	0	4	748
diabetes	diabetes (37)	8	0	8	768
breast-w	breast-w (15)	9	0	9	699
ilpd	ilpd (1480)	9	1	11	583
monks2	monks-problems-2 (334)	0	6	17	601
climate	climate-model-simulation-crashes (40994)	18	0	18	540
kc2	kc2 (1063)	21	0	21	522
pc1	pc1 (1068)	21	0	21	1,109
kc1	kc1 (1067)	21	0	21	2,109
heart	heart-c (982)	6	7	26	303
tictactoe	tic-tac-toe (50)	0	9	27	958
wdbc	wdbc (1510)	30	0	30	569
churn	churn (40701)	16	4	33	5,000
pc3	pc3 (1050)	37	0	37	1,563
biodeg	qsar-biodeg (1494)	41	0	41	1,055
credit	credit-approval (29)	6	9	51	690
spambase	spambase (44)	57	0	57	4,601
credit-g	credit-g (31)	7	13	61	1,000
friedman	fri_c4_500_100 (610)	100	0	100	500
usps	USPS (41964)	256	0	256	1,424
bioresponse	Bioresponse (45019)	419	0	419	3,434
speeddating	SpeedDating (40536)	59	61	503	8,378

TABLE III
 CLASSIFICATION PERFORMANCE OF RO-FIGS ON DATASETS THAT INCLUDE NOMINAL FEATURES, USING THREE DIFFERENT ENCODINGS FOR NOMINAL FEATURES: E-OHE, E-COUNT AND E-PROP. WE REPORT MEAN \pm STD OF THE TEST BALANCED ACCURACY ACROSS 10 FOLDS. ONE-HOT ENCODING (E-OHE) LEADS TO THE BEST PERFORMANCE ON AVERAGE.

Dataset	E-OHE	E-COUNT	E-PROP
ilpd	61.9 \pm 10.4	62.9 \pm 7.7	61.6 \pm 4.2
monks-2	99.5 \pm 0.8	76.5 \pm 6.6	76.2 \pm 4.5
heart	84.8 \pm 6.4	83.5 \pm 6.7	81.8 \pm 5.4
tictactoe	94.4 \pm 3.1	78.1 \pm 4.7	87.5 \pm 3.9
churn	86.3 \pm 2.0	82.3 \pm 3.6	86.7 \pm 2.1
credit	85.7 \pm 5.2	86.7 \pm 3.8	86.2 \pm 3.1
credit-g	65.7 \pm 5.0	65.6 \pm 5.2	66.4 \pm 2.3
Avg. rank	1.7	2.1	2.1

TABLE IV

SEARCH SPACE FOR HYPERPARAMETERS OF TREE-BASED BASELINES. WE USE $\text{HP} \cdot \text{QUNIFORM}$ TO DEFINE THE SPACE UNLESS MARKED OTHERWISE. SYMBOLS $*$, \dagger , AND \star DENOTE THE USE OF $\text{HP} \cdot \text{UNIFORM}$, $\text{HP} \cdot \text{LOGUNIFORM}$, AND $\text{HP} \cdot \text{CHOICE}$, RESPECTIVELY. d DENOTES THE TOTAL NUMBER OF FEATURES PER DATASET.

Method	Hyperparameter	Type	Range
DT	max_depth	Discrete	[1, ..., 30]
	min_samples_leaf	Discrete	[1, ..., 40]
	min_samples_split	Discrete	[2, ..., 40]
MT	alpha *	Continuous	[0.5, ..., 1]
	max_depth	Discrete	[1, ..., 20]
	min_samples_leaf	Discrete	[3, ..., 40]
	min_samples_split	Discrete	[6, ..., 40]
ODT	max_depth	Discrete	[1, ..., 30]
	max_features \star	Choice	[1, 2, \sqrt{d} , $\frac{d}{4}$, $\frac{d}{2}$, d]
	min_examples_to_split	Discrete	[2, ..., 40]
RF	n_estimators	Discrete	[5, ..., 250]
	max_depth	Discrete	[1, ..., 30]
	min_samples_leaf	Discrete	[1, ..., 40]
	min_samples_split	Discrete	[2, ..., 40]
ETC	n_estimators	Discrete	[5, ..., 250]
	max_depth	Discrete	[1, ..., 30]
	min_samples_leaf	Discrete	[1, ..., 40]
	min_samples_split	Discrete	[2, ..., 40]
CatBoost	n_estimators	Discrete	[5, ..., 250]
	max_depth	Discrete	[1, ..., 30]
	learning_rate \dagger	Continuous	[0.01, ..., 0.25]
	num_leaves	Discrete	[2, ..., 40]
	min_child_samples	Discrete	[1, ..., 40]
LightGBM	n_estimators	Discrete	[5, ..., 250]
	max_depth	Discrete	[1, ..., 30]
	learning_rate \dagger	Continuous	[0.01, ..., 0.25]
	num_leaves	Discrete	[2, ..., 40]
	min_child_samples	Discrete	[1, ..., 40]
XGBoost	n_estimators	Discrete	[5, ..., 250]
	max_depth	Discrete	[1, ..., 30]
	learning_rate \dagger	Continuous	[0.01, ..., 0.25]
	min_split_loss	Discrete	[0, ..., 40]
	min_child_weight	Discrete	[1, ..., 40]
FIGS	max_rules	Discrete	[1, ..., 20]
	max_trees	Discrete	[1, ..., 20]
EnsODT	max_depth	Discrete	[1, ..., 30]
	max_features \star	Choice	[1, 2, \sqrt{d} , $\frac{d}{4}$, $\frac{d}{2}$, d]
	min_examples_to_split	Discrete	[2, ..., 40]
	num_trees	Discrete	[5, ..., 50]
MLP	num_epoch	Discrete	[1,000]
	patience	Discrete	[50, ..., 300]
	learning_rate \dagger	Continuous	[0.0001, ..., 0.01]
	dropout_rate *	Continuous	[0, ..., 0.25]
	weight_decay *	Continuous	[0, ..., 0.01]
	L1 *	Continuous	[0, ..., 0.01]

TABLE V

OPTIMAL CONFIGURATION, LEADING TO THE BEST PERFORMANCE ON TEST DATA, IS REPORTED IN THE MIDDLE TWO COLUMNS: MIN_IMP_DEC IS A MINIMUM IMPURITY DECREASE VALUE USED AS A STOPPING CONDITION, AND BEAM_SIZE REPRESENTS THE NUMBER OF FEATURES THAT ARE CONSIDERED PER SPLIT. ALTHOUGH THE OPTIMAL BEAM_SIZE VALUE IS OFTEN LARGE, THE ACTUAL AVERAGE NUMBER OF FEATURES PER SPLIT, REPORTED IN THE LAST COLUMN, IS MUCH LOWER.

Dataset	Optimal		Actual
	MIN_IMP_DEC	BEAM_SIZE	#features per split
blood	5	2	1.6 ± 0.2
diabetes	10	8	3.0 ± 0.0
breast-w	1	9	4.1 ± 0.4
ilpd	0.1	5	2.0 ± 0.0
monks2	0.1	17	7.2 ± 0.5
climate	0.1	18	7.7 ± 0.6
kc2	10	21	10.7 ± 0.8
pc1	0.1	4	1.7 ± 0.1
kc1	0.05	4	2.0 ± 0.1
heart	10	26	9.7 ± 0.7
tictactoe	0.05	13	4.5 ± 0.2
wdbc	1	30	10.4 ± 1.4
churn	5	33	9.6 ± 0.9
pc3	0.1	18	7.4 ± 0.2
biodeg	10	41	14.6 ± 1.7
credit	1	12	3.9 ± 0.5
spambase	0.1	57	31.4 ± 0.5
credit-g	1	2	1.2 ± 0.1
friedman	10	25	9.1 ± 1.3
usps	1	256	46.4 ± 15.2
bioresponse	0.05	419	45.8 ± 13.3
speeddating	10	125	50.1 ± 3.9

APPENDIX B
EXTENDED GENERAL RESULTS

In this section, we provide additional results from Section IV.

A. Performance of additional baselines

We first show additional results of baselines that were excluded in the paper. Table VI compares the performance of three gradient-boosted decision tree methods—CatBoost, LightGBM, and XGBoost—with RO-FIGS. We choose CatBoost as a representative method of the class of gradient-boosted decision trees because it performs the best out of three. Table VII then compares RO-FIGS and TabPFN, which we excluded as a baseline due to potential bias and misleading results; TabPFN was pre-trained on some of the datasets we used for evaluation.

TABLE VI

CLASSIFICATION PERFORMANCE OF LIGHTGBM, XGBOOST, CATBOOST, AND RO-FIGS ON 22 TABULAR DATASETS. WE REPORT MEAN \pm STD OF THE TEST BALANCED ACCURACY ACROSS 10 FOLDS. THE HIGHEST ACCURACY FOR EACH DATASET ACROSS ALL METHODS IS BOLDED, AND THE HIGHEST ACCURACY FOR EACH DATASET ACROSS BASELINES IS UNDERLINED. CATBOOST IS PERFORMING BEST OUT OF THE THREE GRADIENT-BOOSTED DECISION TREE METHODS WITH 12 WINS.

Dataset	LightGBM	XGBoost	CatBoost	RO-FIGS
blood	60.6 \pm 5.5	59.9 \pm 5.6	60.3 \pm 5.8	68.5 \pm 4.1
diabetes	<u>73.1 \pm 5.4</u>	69.5 \pm 5.0	70.5 \pm 7.0	73.6 \pm 4.7
breast-w	95.2 \pm 2.6	94.9 \pm 2.5	<u>95.9 \pm 2.8</u>	96.5 \pm 1.9
ilpd	59.2 \pm 7.7	57.4 \pm 5.3	<u>58.9 \pm 6.8</u>	61.9 \pm 10.4
monks2	<u>98.0 \pm 2.5</u>	98.0 \pm 2.6	78.3 \pm 8.1	99.5 \pm 0.8
climate	<u>71.2 \pm 11.0</u>	68.8 \pm 12.7	68.1 \pm 10.7	73.1 \pm 15.6
kc2	68.8 \pm 6.0	69.0 \pm 7.3	<u>69.2 \pm 7.5</u>	77.6 \pm 7.9
pc1	62.8 \pm 5.4	62.5 \pm 7.9	61.2 \pm 9.4	66.6 \pm 7.2
kc1	<u>63.7 \pm 4.0</u>	66.8 \pm 2.5	65.0 \pm 3.3	64.9 \pm 4.9
heart	82.2 \pm 5.3	82.9 \pm 4.8	<u>83.3 \pm 5.2</u>	84.8 \pm 6.4
tictactoe	99.1 \pm 1.3	97.9 \pm 2.3	99.9 \pm 0.1	94.4 \pm 3.1
wdbc	96.1 \pm 3.0	94.5 \pm 3.5	96.3 \pm 2.4	95.6 \pm 3.5
churn	87.5 \pm 2.3	85.4 \pm 2.4	88.3 \pm 1.9	86.3 \pm 2.0
pc3	60.2 \pm 5.8	59.0 \pm 7.4	<u>60.7 \pm 6.5</u>	62.9 \pm 6.6
biodeg	84.8 \pm 3.4	82.4 \pm 5.7	85.3 \pm 2.7	82.7 \pm 3.7
credit	86.5 \pm 3.9	85.3 \pm 4.2	86.8 \pm 4.4	85.7 \pm 5.2
spambase	94.9 \pm 1.6	93.8 \pm 2.5	94.9 \pm 1.2	92.9 \pm 1.3
credit-g	67.5 \pm 3.1	67.6 \pm 5.4	66.8 \pm 4.9	65.7 \pm 5.0
friedman	88.1 \pm 3.9	<u>87.5 \pm 3.3</u>	86.4 \pm 8.7	80.0 \pm 7.4
usps	97.3 \pm 1.8	96.6 \pm 1.6	98.0 \pm 1.5	97.5 \pm 1.6
bioresponse	78.2 \pm 2.7	77.1 \pm 2.0	<u>77.7 \pm 3.3</u>	72.9 \pm 2.6
speeddating	68.6 \pm 1.4	68.1 \pm 1.4	69.1 \pm 1.9	65.4 \pm 1.9

B. Ablation studies on RO-FIGS

We first compare learning processes in FIGS and RO-FIGS, which extends Fig. 1. Specifically, Fig. 5 highlights the main difference between FIGS and RO-FIGS: the use of univariate and oblique splits, respectively.

Table VIII then demonstrates that utilising the total number of splits as a stopping condition (as in FIGS) leads to subpar performance. This implies that employing the minimum impurity decrease parameter (i.e., MIN_IMP_DEC) as a stopping condition for model growth is recommended over simply limiting the number of splits in the model.

Next, we analyse how oblique splits contribute to performance. In Fig. 6, FIGS, shown as a reference point at 0%, and RO-FIGS correspond to values in Table I. We further investigate how the extreme values of the BEAM_SIZE parameter influence the performance of RO-FIGS models. Namely, RO-FIGS-min and RO-FIGS-max consider one or all available features at each split, respectively. We can see a notable increase in performance when using oblique splits (in both RO-FIGS and RO-FIGS-max), although considering all available features at each step can be suboptimal. Finally, we expect RO-FIGS-min to perform the worst as it randomly picks one feature when creating splits. We observe however that it outperforms FIGS on 11 out of 22 datasets. This suggests that using MIN_IMP_DEC as a stopping condition is sometimes better than simply limiting the maximum number of splits in the model. Note that both methods construct univariate splits.

TABLE VII

CLASSIFICATION PERFORMANCE OF TABPFN AND RO-FIGS ON 22 TABULAR DATASETS. WE REPORT MEAN \pm STD OF THE TEST BALANCED ACCURACY ACROSS 10 FOLDS. THE HIGHEST ACCURACY FOR EACH DATASET ACROSS ALL METHODS IS BOLDED. TABPFN IS A COMPETITIVE AND FAST BASELINE, BUT IT IS NOT SUITABLE FOR DATASETS WITH MORE THAN 100 FEATURES OR 10K SAMPLES (THE LAST THREE ROWS). MOREOVER, IT IS A TRANSFORMER-BASED METHOD AND THUS OFFERS VERY LIMITED INTERPRETABILITY FOR ITS DECISIONS.

Dataset	TabPFN	RO-FIGS
blood	63.5 \pm 4.6	68.5 \pm 4.1
diabetes	72.0 \pm 6.5	73.6 \pm 4.7
breast-w	96.7 \pm 2.0	96.5 \pm 1.9
ilpd	60.5 \pm 5.0	61.9 \pm 10.4
monks2	99.9 \pm 0.1	99.5 \pm 0.8
climate	82.8 \pm 8.2	73.1 \pm 15.6
kc2	69.0 \pm 7.1	77.6 \pm 7.9
pc1	52.5 \pm 4.9	66.6 \pm 7.2
kc1	58.2 \pm 3.1	64.9 \pm 4.9
heart	84.5 \pm 7.1	84.8 \pm 6.4
tictactoe	97.0 \pm 2.1	94.4 \pm 3.1
wdbc	97.7 \pm 2.2	95.6 \pm 3.5
churn	83.5 \pm 2.6	86.3 \pm 2.0
pc3	52.3 \pm 2.3	62.9 \pm 6.6
biodeg	86.8 \pm 4.1	82.7 \pm 3.7
credit	86.2 \pm 4.3	85.7 \pm 5.2
spambase	94.7 \pm 1.1	92.9 \pm 1.3
credit-g	68.5 \pm 4.5	65.7 \pm 5.0
friedman	63.4 \pm 7.3	80.0 \pm 7.4
usps	50.0 \pm 0.0	97.5 \pm 1.6
bioresponse	50.0 \pm 0.0	72.9 \pm 2.6
speeddating	50.0 \pm 0.0	65.4 \pm 1.9

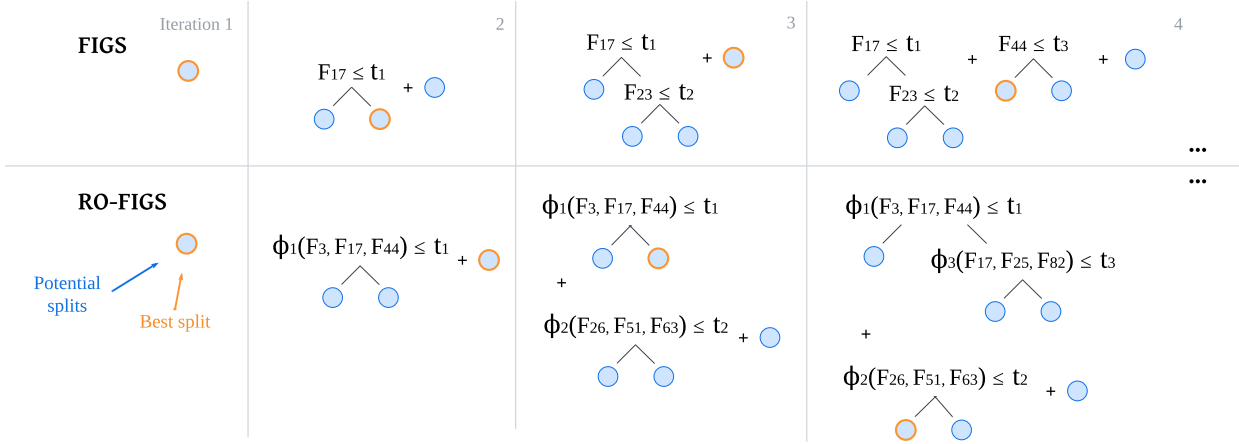


Fig. 5. Comparison of fitting processes of FIGS and RO-FIGS. In each iteration, both methods add one split to the model. However, RO-FIGS computes a linear combination of multiple randomly selected features, while FIGS builds splits with one feature. t , Φ , F denote thresholds, functions, and features, respectively. The figure has been adapted from [10].

TABLE VIII

PERFORMANCE COMPARISON OF RO-FIGS WITH DIFFERENT STOPPING CONDITIONS: RO-FIGS-SPLITS USES THE TOTAL NUMBER OF SPLITS (I.E., MAX_SPLITS, RESTRICTED TO 20 LIKE FIGS), WHILE RO-FIGS EMPLOYS THE MINIMUM IMPURITY DECREASE CONDITION (I.E., MIN_IMP_DEC). BOTH CONFIGURATIONS REPRESENT THE OPTIMAL SETUP. WE REPORT THE MEAN \pm STD OF THE TEST BALANCED ACCURACY ACROSS 10 FOLDS IN THE MIDDLE TWO COLUMNS, WHILE THE LAST COLUMN SHOWS THE RELATIVE INCREASE IN PERFORMANCE OF RO-FIGS OVER RO-FIGS-SPLITS. RO-FIGS, GUIDED BY THE MINIMUM IMPURITY DECREASE, EXHIBITS SUPERIOR ACCURACY. NOTABLY, THE HIGHEST PERFORMANCE INCREASE OF 9.7% IS SEEN ON THE *kc2* DATASET.

Dataset	RO-FIGS-splits	RO-FIGS	Increase (%)
blood	62.7 \pm 6.4	68.5 \pm 4.1	5.8
diabetes	72.6 \pm 6.4	73.6 \pm 4.7	1.0
breast-w	96.0 \pm 2.0	96.5 \pm 1.9	0.5
ilpd	59.1 \pm 5.0	61.9 \pm 10.4	2.8
monks2	99.5 \pm 0.8	99.5 \pm 0.8	0.0
climate	72.0 \pm 15.9	73.1 \pm 15.6	1.1
kc2	67.9 \pm 6.1	77.6 \pm 7.9	9.7
pc1	62.9 \pm 5.6	66.6 \pm 7.2	3.7
kc1	60.7 \pm 4.3	64.9 \pm 4.9	4.2
heart	82.4 \pm 7.6	84.8 \pm 6.4	2.4
tictactoe	91.5 \pm 3.9	94.4 \pm 3.1	2.9
wdbc	95.6 \pm 3.4	95.6 \pm 3.5	0.0
churn	85.5 \pm 1.8	86.3 \pm 2.0	0.8
pc3	59.1 \pm 6.1	62.9 \pm 6.6	3.8
biodeg	82.6 \pm 2.9	82.7 \pm 3.7	0.1
credit	85.3 \pm 3.8	85.7 \pm 5.2	0.4
spambase	92.7 \pm 1.5	92.9 \pm 1.3	0.2
credit-g	64.8 \pm 4.2	65.7 \pm 5.0	0.9
friedman	76.0 \pm 5.9	80.0 \pm 7.4	4.0
usps	97.7 \pm 1.6	97.5 \pm 1.6	-0.2
bioresponse	72.9 \pm 2.6	72.9 \pm 2.6	0.0
speeddating	66.0 \pm 1.6	65.4 \pm 1.9	-0.6

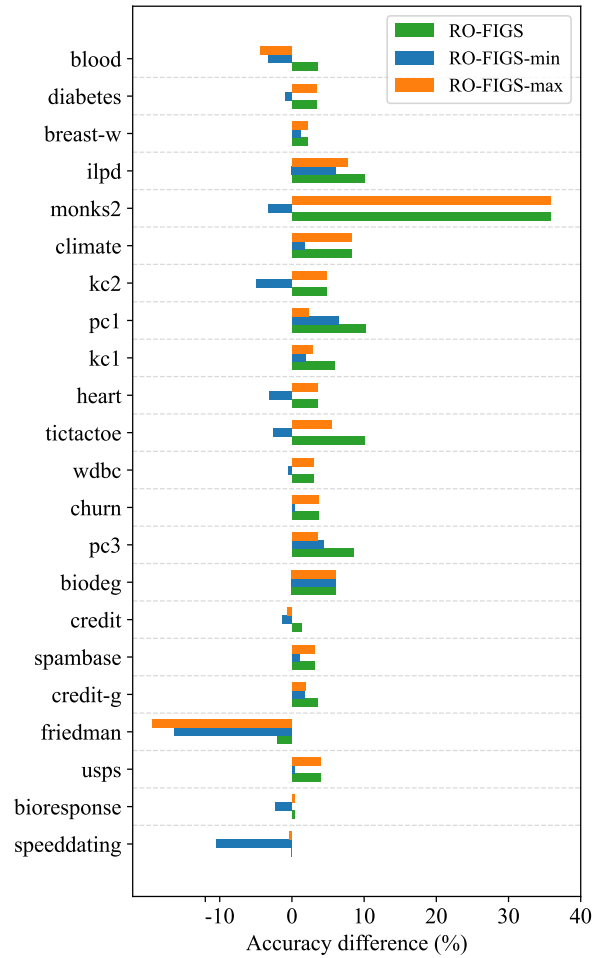


Fig. 6. The effect of oblique splits on the mean balanced accuracy across 10 folds. We use the FIGS baseline with univariate splits as a reference point (with an accuracy difference of 0%). Each bar illustrates the difference in performance between FIGS and the corresponding method, where a positive difference indicates higher accuracy. RO-FIGS represents the optimal configuration of RO-FIGS, while RO-FIGS-min and RO-FIGS-max represent RO-FIGS models with BEAM_SIZE set to extreme values, that is, one and all. There is a clear improvement in accuracy when using oblique splits, but note that using all available features can be suboptimal.

C. Efficiency

Tables IX and X show the number of trees and splits for the tree-based methods, respectively. They demonstrate that RO-FIGS models are compact and significantly smaller than the standard tree-based ensembles such as random forest and CatBoost. In terms of size, RO-FIGS models are most comparable to FIGS (limited to 20 splits) but exhibit much better performance (see Table D).

TABLE IX

THE NUMBER OF TREES BUILT BY TREE-BASED METHODS. WE LEAVE OUT METHODS THAT BUILD EXACTLY ONE TREE AND REPORT THE MEAN \pm STD OF THE NUMBER OF TREES ON THE TEST SET ACROSS 10 FOLDS. RO-FIGS BUILDS MULTIPLE TREES WHEN THE UNDERLYING DATA HAS AN ADDITIVE STRUCTURE PRESENT, AND THIS ALMOST ALWAYS COINCIDES WITH FIGS FINDING THE ADDITIVE STRUCTURE AS WELL. THE NUMBER OF TREES IN RO-FIGS MODELS IS UNSURPRISINGLY MUCH LOWER THAN THE NUMBER OF TREES IN ENSEMBLES AND COMPARABLE TO THAT OF FIGS.

Dataset	RF	ETC	CatBoost	FIGS	EnsODT	RO-FIGS
blood	73.4 \pm 51.2	135.4 \pm 71.6	78.0 \pm 78.0	1.0 \pm 0.0	24.8 \pm 10.4	1.0 \pm 0.0
diabetes	96.1 \pm 70.0	143.4 \pm 76.7	59.0 \pm 39.8	1.6 \pm 0.7	29.7 \pm 17.7	1.0 \pm 0.0
breast-w	41.3 \pm 57.7	47.1 \pm 58.7	47.8 \pm 46.0	1.0 \pm 0.0	18.6 \pm 12.9	1.0 \pm 0.0
ilpd	60.7 \pm 58.0	151.5 \pm 70.6	169.5 \pm 89.0	1.8 \pm 0.6	18.7 \pm 11.6	3.0 \pm 0.8
monks2	184.3 \pm 15.2	176.6 \pm 18.9	230.6 \pm 19.4	1.0 \pm 0.0	28.4 \pm 10.9	2.3 \pm 1.1
climate	71.5 \pm 73.5	9.0 \pm 0.0	120.9 \pm 57.2	1.1 \pm 0.3	19.6 \pm 14.7	2.0 \pm 0.9
kc2	57.5 \pm 78.0	84.0 \pm 100.8	73.1 \pm 65.5	1.0 \pm 0.0	23.0 \pm 8.8	1.0 \pm 0.0
pc1	50.0 \pm 58.4	109.9 \pm 80.5	91.1 \pm 75.5	1.6 \pm 0.7	25.2 \pm 14.5	2.4 \pm 1.0
kc1	64.5 \pm 66.6	93.1 \pm 85.3	111.7 \pm 66.3	1.3 \pm 0.5	27.1 \pm 17.6	1.4 \pm 0.5
heart	49.7 \pm 71.8	68.4 \pm 46.1	53.8 \pm 52.3	3.1 \pm 1.5	23.6 \pm 13.9	1.0 \pm 0.0
tictactoe	173.5 \pm 27.0	148.2 \pm 60.6	214.0 \pm 5.6	4.5 \pm 2.7	41.2 \pm 5.7	4.9 \pm 1.3
wdbc	28.5 \pm 38.3	45.9 \pm 50.1	68.0 \pm 45.1	1.0 \pm 0.0	24.1 \pm 12.6	1.0 \pm 0.0
churn	186.6 \pm 21.8	175.4 \pm 8.2	92.8 \pm 68.3	1.8 \pm 0.8	26.8 \pm 13.8	1.1 \pm 0.3
pc3	94.2 \pm 64.1	97.4 \pm 93.1	124.0 \pm 60.7	1.5 \pm 0.5	14.9 \pm 11.9	1.8 \pm 0.9
biodeg	61.1 \pm 46.9	114.3 \pm 75.6	105.4 \pm 86.0	2.1 \pm 0.9	35.0 \pm 14.8	1.0 \pm 0.0
credit	97.3 \pm 55.1	47.9 \pm 69.5	49.2 \pm 47.1	1.4 \pm 0.7	25.0 \pm 13.0	1.0 \pm 0.0
spambase	37.1 \pm 29.6	162.9 \pm 56.9	79.1 \pm 44.0	2.5 \pm 1.4	19.1 \pm 11.1	2.9 \pm 0.7
credit-g	156.9 \pm 60.6	151.1 \pm 65.4	131.7 \pm 81.1	1.6 \pm 1.0	31.3 \pm 16.1	4.6 \pm 1.2
friedman	118.6 \pm 49.4	130.5 \pm 76.3	143.8 \pm 95.1	1.5 \pm 0.5	24.9 \pm 8.2	1.2 \pm 0.4
usps	27.7 \pm 18.7	27.6 \pm 17.1	70.8 \pm 67.1	1.0 \pm 0.0	28.0 \pm 8.2	1.0 \pm 0.0
bioresponse	188.5 \pm 33.7	144.9 \pm 64.3	137.9 \pm 66.7	2.7 \pm 1.1	34.9 \pm 11.2	2.0 \pm 0.7
speeddating	53.9 \pm 72.8	143.0 \pm 72.9	178.3 \pm 71.5	2.6 \pm 1.0	23.7 \pm 9.6	2.6 \pm 0.5

TABLE X

THE NUMBER OF SPLITS IN TREE-BASED MODELS. WE REPORT THE MEAN \pm STD OF THE NUMBER OF SPLITS ON THE TEST SET ACROSS 10 FOLDS. RO-FIGS HAS A SURPRISINGLY LOW NUMBER OF SPLITS ON SOME DATASETS (E.G., *diabetes*, *kc2*, *heart*) AND IS COMPARABLE TO SINGLE DECISION TREES AND FIGS MODELS.

Dataset	DT	MT	OT	ODT	RF	ETC	CatBoost	FIGS	EnsODT	RO-FIGS
blood	29.5 \pm 18.1	7.5 \pm 3.9	7.0 \pm 0.0	12.9 \pm 6.5	1710.2 \pm 1600.9	11192.1 \pm 7989.8	1082.1 \pm 976.4	6.7 \pm 5.4	348.1 \pm 143.6	2.0 \pm 0.0
diabetes	31.1 \pm 19.1	19.6 \pm 5.6	7.0 \pm 0.0	21.6 \pm 19.0	4461.5 \pm 3693.3	13844.3 \pm 8236.0	978.0 \pm 1003.8	7.1 \pm 4.4	805.1 \pm 697.5	1.0 \pm 0.0
breast-w	9.6 \pm 3.9	6.1 \pm 1.7	7.0 \pm 0.0	7.4 \pm 5.2	242.0 \pm 346.4	746.5 \pm 1181.3	583.2 \pm 1080.4	8.4 \pm 6.1	92.1 \pm 79.5	4.6 \pm 1.6
ilpd	16.3 \pm 7.8	17.0 \pm 6.3	7.0 \pm 0.0	13.9 \pm 6.2	1356.9 \pm 1726.4	13946.2 \pm 7690.0	2399.6 \pm 2449.8	11.9 \pm 6.9	376.0 \pm 284.4	75.0 \pm 0.0
monks2	43.5 \pm 6.4	12.3 \pm 2.9	7.0 \pm 0.0	16.9 \pm 9.7	12997.4 \pm 3299.3	17884.9 \pm 7510.0	6439.9 \pm 895.7	17.6 \pm 3.1	428.8 \pm 221.3	11.5 \pm 5.6
climate	10.4 \pm 4.4	7.7 \pm 1.8	7.0 \pm 0.0	9.3 \pm 3.8	1153.5 \pm 1368.3	9.0 \pm 0.0	970.5 \pm 362.3	7.1 \pm 3.3	124.3 \pm 104.4	14.3 \pm 5.3
kc2	9.8 \pm 10.1	4.2 \pm 2.0	7.0 \pm 0.0	13.8 \pm 12.5	505.4 \pm 1029.1	3520.7 \pm 4598.1	1312.7 \pm 2038.7	4.3 \pm 4.2	305.2 \pm 172.9	1.0 \pm 0.0
pc1	21.9 \pm 10.0	3.5 \pm 1.4	7.0 \pm 0.0	21.0 \pm 12.1	1352.1 \pm 2298.3	9208.8 \pm 7772.3	1584.7 \pm 1249.0	9.6 \pm 6.9	530.8 \pm 356.5	61.7 \pm 10.3
kc1	70.4 \pm 39.5	13.1 \pm 2.9	7.0 \pm 0.0	18.3 \pm 14.4	5047.0 \pm 8846.3	20019.2 \pm 24310.8	2254.7 \pm 1343.0	12.1 \pm 5.7	1160.6 \pm 1103.8	75.0 \pm 0.0
heart	8.2 \pm 4.6	9.9 \pm 1.8	7.0 \pm 0.0	9.9 \pm 5.2	557.7 \pm 1354.8	667.5 \pm 455.6	742.7 \pm 1659.3	7.0 \pm 5.3	232.0 \pm 188.2	1.0 \pm 0.0
tictactoe	32.8 \pm 14.6	0.0 \pm 0.0	7.0 \pm 0.0	29.4 \pm 10.0	17075.7 \pm 7980.9	16977.5 \pm 8817.3	4787.6 \pm 1135.9	18.8 \pm 1.2	1072.4 \pm 244.4	74.7 \pm 0.9
wdbc	5.9 \pm 2.9	7.4 \pm 3.5	7.0 \pm 0.0	4.9 \pm 6.5	250.8 \pm 309.9	982.7 \pm 1657.8	650.7 \pm 543.4	5.0 \pm 3.0	177.5 \pm 180.2	3.3 \pm 1.6
churn	89.9 \pm 47.5	53.4 \pm 23.6	7.0 \pm 0.0	54.9 \pm 31.3	29896.6 \pm 3760.8	50553.5 \pm 6254.8	1539.1 \pm 680.9	16.5 \pm 3.4	1939.1 \pm 1195.6	7.6 \pm 1.5
pc3	46.5 \pm 18.4	22.4 \pm 5.9	7.0 \pm 0.0	31.9 \pm 18.3	4160.6 \pm 3864.9	12664.5 \pm 13116.7	2374.8 \pm 2167.2	12.7 \pm 5.8	508.4 \pm 488.7	74.6 \pm 1.3
biodeg	28.6 \pm 13.9	22.1 \pm 10.2	7.0 \pm 0.0	20.5 \pm 18.1	2963.5 \pm 2593.0	10230.1 \pm 8861.9	1454.1 \pm 1161.7	12.4 \pm 7.8	1271.8 \pm 1085.7	1.5 \pm 0.5
credit	17.1 \pm 11.9	17.8 \pm 3.0	7.0 \pm 0.0	16.1 \pm 11.7	2166.9 \pm 2690.3	472.6 \pm 289.9	1446.3 \pm 1623.7	4.8 \pm 5.2	347.3 \pm 226.8	1.0 \pm 0.0
spambase	69.8 \pm 41.1	34.7 \pm 12.8	7.0 \pm 0.0	32.5 \pm 16.6	3294.5 \pm 1900.7	41196.7 \pm 19747.7	1057.7 \pm 302.1	16.2 \pm 2.7	1152.7 \pm 770.1	67.1 \pm 9.6
credit-g	46.3 \pm 23.4	21.5 \pm 2.0	7.0 \pm 0.0	29.9 \pm 25.4	14847.1 \pm 10333.6	21764.1 \pm 19358.2	1922.3 \pm 1344.5	12.3 \pm 4.1	934.2 \pm 983.3	33.0 \pm 5.7
friedman	14.7 \pm 8.7	3.2 \pm 0.4	7.0 \pm 0.0	13.8 \pm 7.1	3213.1 \pm 2491.3	8503.3 \pm 6733.3	1423.5 \pm 1036.9	8.1 \pm 3.4	407.9 \pm 204.5	3.5 \pm 1.1
usps	20.0 \pm 7.0	2.5 \pm 0.5	7.0 \pm 0.0	3.3 \pm 2.7	563.5 \pm 343.2	1635.4 \pm 1455.6	651.2 \pm 480.3	12.8 \pm 6.0	280.6 \pm 277.6	2.4 \pm 0.8
bioresponse	52.9 \pm 18.4	63.7 \pm 7.7	7.0 \pm 0.0	74.1 \pm 84.7	37456.3 \pm 11098.1	40008.3 \pm 25743.0	2113.2 \pm 1808.4	12.0 \pm 5.2	3145.8 \pm 2438.1	5.1 \pm 2.0
speeddating	101.5 \pm 67.6	38.0 \pm 4.0	7.0 \pm 0.0	67.3 \pm 42.0	17446.1 \pm 26780.3	103295.8 \pm 64515.4	4255.5 \pm 2865.4	7.2 \pm 4.6	2187.7 \pm 1208.7	13.1 \pm 2.8

D. Expressiveness

Here, we further discuss the expressiveness of the RO-FIGS models. Due to the robustness of tree-based models to uninformative features, feature importance information is often extracted from them. To extract such information from RO-FIGS models, we first count combinations of features that appear together in the splits. We then analyse this jointly with the SHAP summary plot, which illustrates how each feature contributed to the model. Next, we analyse SHAP plots of baseline methods. In particular, we choose FIGS due to its similarity to RO-FIGS (w.r.t. the framework and size of the models), and CatBoost as the best-performing baseline.

Figs. 7 and 8 present SHAP summary plots for RO-FIGS, FIGS, and CatBoost models on two datasets, *diabetes* and *blood*, respectively. Note that these plots are computed on fold 0, but similar behaviour is observed across all folds. Shap values are estimated using Kernel SHAP, where the `nsamples` parameter is set to 100. Furthermore, we utilise `shap.sample` to generate a background summary with 100 samples.

We observe that the oblique nature of splits in RO-FIGS reflect feature interactions, which makes them more expressive than models with univariate trees. Furthermore, such insights cannot be learnt from feature importance tools such as SHAP. For example, on the *diabetes* dataset, RO-FIGS builds models with only one split involving a linear combination of three features. Similarly, on the *blood* dataset, RO-FIGS model consists of two splits, one of which is a linear combination of two features *monetary* and *time*.

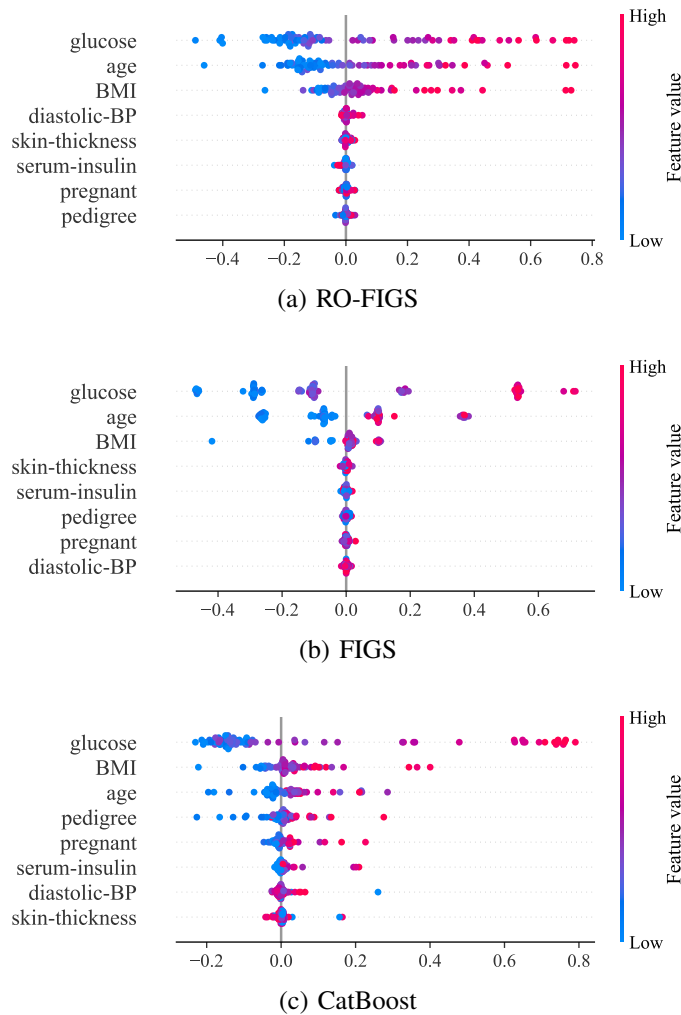


Fig. 7. SHAP summary plots of different models on the first fold of the *diabetes* dataset all implicate that features *glucose*, *age*, and *BMI* contribute to their predictions the most. RO-FIGS with the accuracy of 73.6% (see Table I) outperforms all baselines on this dataset with only one split, demonstrating that a linear combination of features *glucose*, *age*, and *BMI* is optimal.

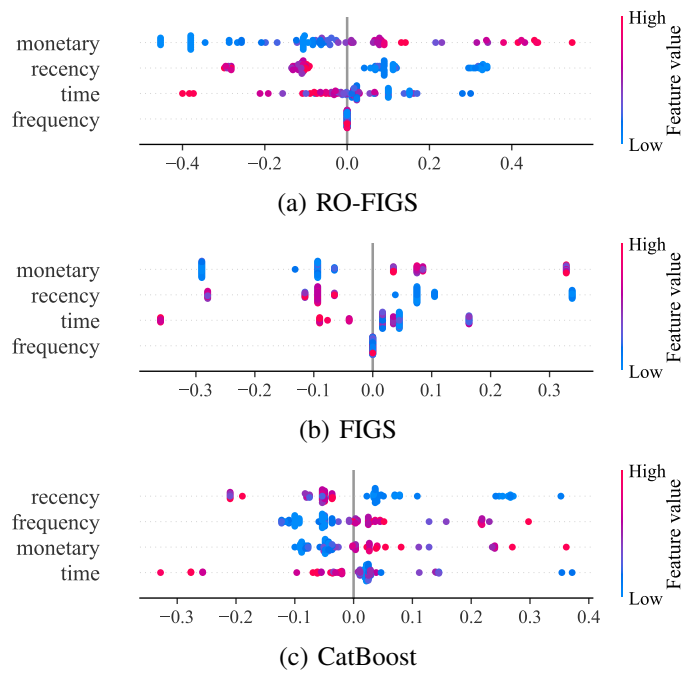


Fig. 8. The same as Fig. 7 but on the *blood* dataset. Three methods generally disagree on the importance of features: neither of the FIGS-based models split on *frequency*, but this feature is the second most important for CatBoost. With only 2 splits, one using *recency* and the other a linear combination of *monetary* and *time*, RO-FIGS is able to highlight combinations of features. It also outperforms all baselines, suggesting that this is a highly informative combination of features.